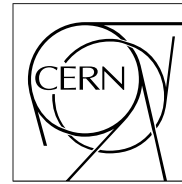


The Compact Muon Solenoid Experiment

CMS Note

Mailing address: CMS CERN, CH-1211 GENEVA 23, Switzerland



May 27, 1999

On b- and τ -multiplicities per event in SUSY (mSUGRA) and instrumental implications

S. Abdullin ^{a)}
 IReS, Strasbourg, France.

D. Denegri ^{b)}
 Centre d'Etudes Nucléaire de Saclay, Gif-sur-Yvette, France

Abstract

We investigate the probability to find a b or τ in SUSY production with the mSUGRA model. We find that in the entire parameter space the probability per event to find a b-jet of $E_T^b > 50$ GeV within CMS acceptance ($|\eta| < 2.4$) is significant for all $\tan\beta$, varying from a ~ 10 % level to 90 % depending on the m_0 , $m_{1/2}$ region. The multiplicity of b-jets per event slightly increases with $\tan\beta$. The probabilities per event to find a τ with the same kinematical cuts is also significant, particularly in the region $m_{1/2} > (1 - 1.5) \cdot m_0$, and it increases sharply with $\tan\beta$. These findings point to the central role a microvertex device would play in case that SUSY (mSUGRA) is indeed realized in nature and found at the LHC. As the m_0 , $m_{1/2}$ parameter space of largest τ and largest b-jet probability per event tend to be complementary, to have an efficient high-performance three-layered microvertex device would be very sound and safe instrumental strategy in this context. First investigations done in the context of the more general MSSM scenario confirm the findings based on mSUGRA.

^{a)} On leave from ITEP, Moscow, Russia. Email: adullin@mail.cern.ch

^{b)} Email: Daniel.Denegri@cern.ch

1 Introduction

One of the main purposes of the LHC collider is to search for the physics beyond the Standard Model (SM). One of the direction of this search is to look for superpartners of ordinary particles expected in Supersymmetric extensions of SM (SUSY). SUSY, if it exists, is expected to reveal itself at LHC firstly via an excess of (multilepton +) multijet + E_T^{miss} final states compared to Standard Model (SM) expectations [1]. Spectacular and revealing structures are also possible in l^+l^- spectra indicative of SUSY production [2]. It has been known for a long time that SUSY production will be accompanied by an excess of b-jets, in part as \tilde{t}_1 and \tilde{b}_1 are expected to be the lightest among the squarks. Recently [3] it has also been shown that with increasing $\tan\beta$ we should expect substantial increase of sparticle branching ratios to third generation particles due to increase of b and τ Yukawa couplings. This implies a significant increase of the τ yield for large $\tan\beta$. Both b's and τ 's require a specific detection technique, relying mostly on precision measurements of impact parameters.

The main goal of this study is to show the importance of good b-jet and tau detection in CMS [4] for SUSY measurements. The importance of b-tagging in $h \rightarrow b\bar{b}$ detection is discussed in [5, 6].

We are interested in evaluating the richness of b-production in SUSY, whose detection relies on microvertexing, and of τ production which requires calorimeter, tracker [7] and microvertexing selection. More emphasis is given to τ production as less known and documented, especially at high $\tan\beta$, but b-production is more rewarding and instrumentally more demanding as it depends on a detection of several fairly soft ($\sim 1 - 5$ GeV/c) tracks with significant impact parameters in a jetty environment.

The paper is organized as follows. We discuss the specific SUSY model employed in section 2. Phenomenological differences of low and high $\tan\beta$ values are briefly discussed in section 3. Then in section 4 the difference between various domains of $m_0, m_{1/2}$ plane for the same $\tan\beta=35$ is discussed. The mSUGRA observations at high $\tan\beta$ are somewhat generalized in case of the minimal extension of the SM (MSSM) in section 5. The main results of this study are summarized in section 6.

2 Model employed

The large number of SUSY parameters, even in the minimal extension of the SM (MSSM), makes it difficult to comprehend the variety of possible signals and signatures and to evaluate the reach in various sparticle searches in general. So, to have a better grasp of the situation, we limit ourselves at present basically to the mSUGRA-MSSM model, except for some specific cases explicitly mentioned. This model emanates from the MSSM, using Grand Unification Theory (GUT) assumptions to limit the number of parameters (see more details in e.g. [8]).

The mSUGRA model contains only five free parameters :

- a common gaugino mass ($m_{1/2}$) ;
- a common scalar mass (m_0);
- a common trilinear interaction amongst the scalars (A_0);
- the ratio of the vacuum expectation values of the Higgs fields that couple to $T_3 = 1/2$ and $T_3 = -1/2$ fermions ($\tan\beta$);
- a Higgsino mixing parameter μ which enters only through its sign ($sign(\mu)$).

For a given choice of model parameters all the masses and couplings, and thus production cross sections (up to structure function) and decay branching ratios are fixed.

The mass of the lightest SUSY particle (LSP) which is $\tilde{\chi}_1^0$ in the R-parity conserving mSUGRA equals approximately $\sim 1/2$ of the $\tilde{\chi}_2^0$ mass. The mass of lightest chargino $\tilde{\chi}_1^\pm$ is almost the same as that of the $\tilde{\chi}_2^0$. Isomass contours of $\tilde{\chi}_{1,2}^0$ and $\tilde{\chi}_1^\pm$ and gluino behave gaugino-like, i.e. depend mainly on $m_{1/2}$. Masses of sleptons and squarks depend on both m_0 and $m_{1/2}$.

Masses of squarks (especially of the first generation), gluinos, charginos and neutralinos depend only weakly on $\tan\beta$, A_0 or $sign(\mu)$ parameters. Masses of sleptons, stop and sbottom have some dependence on these mSUGRA parameters, in particular third generation sparticles on $\tan\beta$; masses of $\tilde{\tau}_1$, \tilde{t}_1 and \tilde{b}_1 tend to be the lightest among the sleptons and squarks respectively with increasing $\tan\beta$. Masses of Higgs bosons depend significantly on $\tan\beta$, the mass of the lightest scalar Higgs h increases with $\tan\beta$ and depends also on $sign(\mu)$, whilst masses of the heavy Higgses decrease dramatically with increasing $\tan\beta$ in this model [3].

Since masses and couplings, thus branchings and cross-sections vary most rapidly with m_0 , $m_{1/2}$, it is natural to follow the commonly used way of presenting mSUGRA searches as a function of these two parameters for different fixed values of $\tan\beta$ and $\text{sign}(\mu)$. The A_0 parameter is usually set to zero, since its variation has only a moderate effect on the results.

In Figs.1,2 one can see total mSUGRA production cross-section (including associated $\tilde{\chi}\tilde{g}$, $\tilde{\chi}\tilde{q}$ and chargino-neutralino pair production) as a function of m_0 , $m_{1/2}$ for chosen sets of $\tan\beta$ and $\text{sign}(\mu)$. The contribution of strongly interacting SUSY particles cross-sections ($\tilde{g}\tilde{g}$, $\tilde{g}\tilde{q}$, $\tilde{q}\tilde{q}$) is also shown separately by dashed lines. The jitter in the contours is caused by limited statistics. The total cross-section for the same values of m_0 , $m_{1/2}$ but for different values of $\tan\beta$ and $\text{sign}(\mu)$ differs slightly. The bulk of the total cross-section for low values of $m_{1/2}$ comes from $\tilde{g}\tilde{g}$, $\tilde{g}\tilde{q}$, $\tilde{q}\tilde{q}$, whereas in the domains with extremely high masses of \tilde{g} , \tilde{q} the contribution of production of squarks or gluinos associated with much lighter (at the same m_0 , $m_{1/2}$) charginos and neutralinos, or even just chargino-neutralino pair production may dominate. The shaded regions along the axes denote theoretically (TH) and up to now experimentally (EX) excluded regions of parameter space as given in the ref. [9].

All the results of this study are obtained with calculations made with ISAJET 7.32, 7.44 generators [10] and modified supplements therein.

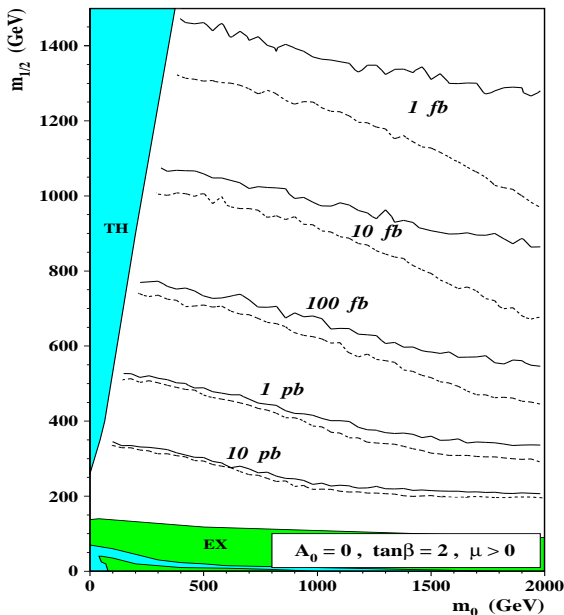


Figure 1: Total mSUGRA cross-section contours as a function of m_0 , $m_{1/2}$ for $A_0 = 0$, $\tan\beta = 2$, $\mu > 0$ (solid line). The contribution of $\tilde{g}\tilde{g}$, $\tilde{g}\tilde{q}$, $\tilde{q}\tilde{q}$ production alone is shown by dashed line.

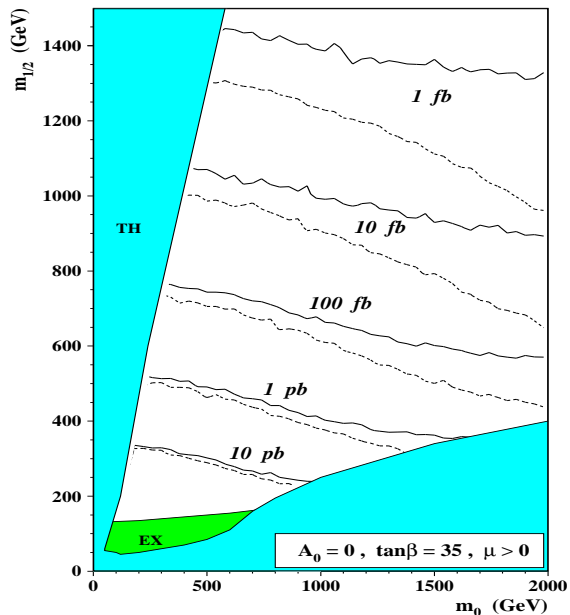


Figure 2: Same as Fig.1, except for $\tan\beta=35$.

3 Difference in phenomenology between low and high values of $\tan\beta$.

Fig.3 a) shows the dependence of mass values of left selectron (\tilde{e}_L) and the lightest tau ($\tilde{\tau}_1$) as a function of $\tan\beta$ at a representative point of mSUGRA parameter space. In Fig.3 b) one sees the dramatic increase of the branching ratios of lightest chargino ($\tilde{\chi}_1^\pm$, dashed line) and next-to-lightest neutralino ($\tilde{\chi}_2^0$, solid line) into final states with lightest tau with increasing $\tan\beta$, due to the increase of the tau Yukawa couplings. This causes the enhancement of final states with taus at large $\tan\beta$. Similar examples of masses and branching ratios dependence on $\tan\beta$ for lower values of m_0 and $m_{1/2}$ (Tevatron range) can be found in ref. [3].

Let us consider in more detail the taus, taking now for example the decay of a heavy gluino in the appropriate domain of parameter space, and compare the abundance of taus in the final states to see the

difference between large and small $\tan\beta$. Figs.4 and 5 show the decay schemes of heavy gluinos and squarks at high $\tan\beta$, whilst Figs.6 and 7 are for low $\tan\beta$. In Fig.4, for $\tan\beta=35$, $\tilde{\chi}_2^0$ and $\tilde{\chi}_1^\pm$ branching ratios for decays into $\tilde{\tau}_{1,2}$ $\tau(\nu)$ exceed 60 %. To simplify the figure, similar intermediate states were grouped. For instance, states $\tilde{\chi}_2^\pm Wbb$ and $\tilde{\chi}_2^\pm tb$ were treated (summed up) as the same, though they have different kinematics in principle (see the rightmost circular mark at $\tilde{\chi}_2^\pm$ horizontal line (1067 GeV). It is almost impossible to follow and calculate all the branchings in gluino decays; some small ones are not shown, thus resulting in a small underestimate of the “final” states (at the level of $\tilde{\chi}_1^0$) branching ratios. The ten final states having the highest branching ratios are listed in the lower part of Figs.4 – 7. The right squarks (\tilde{q}_R) decay entirely into $\tilde{\chi}_1^0$ q final state in the domain of mSUGRA parameter space where $m_{\tilde{q}_R} < m_{\tilde{g}}$ as it is in the point presented in Figs.4 – 7.

In case of low $\tan\beta=2$, Fig.6, the decay chains of gluinos are not so complicated as in case of high $\tan\beta$, Fig.4, mainly due to the fact that $m_{\tilde{t}_1} < m_{\tilde{\chi}_2^\pm, \tilde{\chi}_{3,4}^0}$. Right squarks again, as for high $\tan\beta$, decay entirely into LSP + quarks. In addition, at low $\tan\beta$ the $\tilde{\tau}_{1,2}$ do not dominate in the decays of $\tilde{\chi}_1^\pm$ and $\tilde{\chi}_2^0$, instead, branchings of $\tilde{\chi}_1^\pm$ and $\tilde{\chi}_2^0$ decays into selectrons and smuons are enhanced. Thus final states of gluinos and squarks contain more leptons (e, μ) in case of low $\tan\beta$ than in case of high $\tan\beta$ in the chosen point of mSUGRA parameter space, as also discussed in [11].

What is evident from the list of dominant decay modes at the bottom of Figs.4 – 7 is that b’s are abundantly produced and more so at large $\tan\beta$, but what is striking is the large number of final states containing τ ’s and multiple τ ’s at large $\tan\beta$, providing in fact a method to constrain $\tan\beta$ [11]. Our aim here is to emphasize the instrumental implications of these observations.

4 Differences between various domains of m_0 , $m_{1/2}$ plane for high $\tan\beta$

Let us now consider 5 very different points in the $(m_0, m_{1/2})$ plane for fixed values of $\tan\beta = 35$, $\mu > 0$ and $A_0=0$ (see Table 1). One can see that at the first point (130,240) moderately above the Tevatron II reach, and at the second point (400,900), this latter one already shown in Figs.3 – 5, there is an abundant production of taus, whilst multiple b-jets originate mainly from stop/sbottom production and partly from gluino (it is relatively heavy to contribute significantly to the total cross-section). Some difference in the mass values between Table 1 and Figs.3 – 5 is due to the fact that values in Table 1 are obtained with ISAJET 7.44, whilst those in Figs.3 – 5 are calculated with ISAJET 7.32.

The third point (700,600) is characterized by an increase of b-production due to production of not so heavy gluino, but mainly from $\tilde{\chi}_2^0$. At the same time one can see a drastic decrease of tau production at the third parameter space point, the remaining source of them being the decay of W-bosons and, to some extent, decays of B-mesons.

At the forth point with relatively light gluino and squarks (slightly above the Tevatron II reach, as the first point) τ production is moderate due to smaller branchings of $\tilde{\chi}_2^0$ and $\tilde{\chi}_1^\pm$, whilst b-production is significant (comparable to that at the previous point), despite $\tilde{\chi}_2^0 \rightarrow \tilde{\chi}_1^0 h \rightarrow \tilde{\chi}_1^0 b\bar{b}$ being kinematically forbidden, but there is a large $\tilde{\chi}_2^0$ 3-body decay with $\text{Br}(\tilde{\chi}_2^0 \rightarrow \tilde{\chi}_1^0 b\bar{b}) \approx 23$ %. This is due to the fact that at this point the gluino mass is smaller than masses of squarks (except \tilde{t}_1) and branching ratios of squark decays into gluino + quark are significant, even right squarks now decay mostly through gluino + quark. In turn, the $\text{Br}(\tilde{g} \rightarrow \tilde{b}_1 b) \approx 88$ % at this point.

At the fifth point (1000,400) again the gluino mass is smaller than masses of squarks (except \tilde{t}_1) and squarks mostly decay through gluino + quark. In addition, $\tilde{\chi}_2^0 \rightarrow \tilde{\chi}_1^0 h \rightarrow \tilde{\chi}_1^0 b\bar{b}$ is kinematically allowed, though the yield of $\tilde{\chi}_2^0$ is lower than at point 3 because left squarks often decay via gluino + quark, and $\text{Br}(\tilde{q}_L \rightarrow \tilde{\chi}_2^0 q)$ is only ≈ 17 % against ≈ 32 % at point 3. It results in a significant b-production, since branching of gluino decay into top/bottom final state remains high (≥ 80 %). It also leads to a slight increase of tau production at this point (via $t \rightarrow Wb \rightarrow \tau\nu b$). To conclude this brief overview, b-jets are abundantly produced over most of the m_0 , $m_{1/2}$ plane, i.e. from the Tevatron reach up to the maximal LHC \tilde{g} , \tilde{q} mass reach, whilst τ ’s are abundant in the region $m_{1/2} > (1 - 1.5) \cdot m_0$.

To give a feeling about the situation for “intermediate” $\tan\beta$, we show in Table 2 the masses and branching ratios for the same 5 $(m_0, m_{1/2})$ points as in Table 1, but for $\tan\beta=10$. The only essential difference between the two tables (two values of $\tan\beta$) is in the lower branchings of $\tilde{\chi}_2^0$, $\tilde{\chi}_1^\pm$ decays into $\tilde{\tau}_{1,2}\tau$ and $\tilde{\tau}_{1,2}\nu$ respectively for $\tan\beta=10$.

Table 1: Characteristic features of 5 mSUGRA points. High $\tan\beta$ case .

| Mass of sparticles (GeV) or Branchings (%) | $(m_0, m_{1/2})$ values for $\tan\beta = 35, \mu > 0, A_0=0$ | | | | |
|--|--|----------------|----------------|----------------|-----------------|
| | 1 (130,240) | 2 (400,900) | 3 (700,600) | 4 (500,200) | 5 (1000,400) |
| \tilde{g} | 598 | 2011 | 1407 | 537 | 1010 |
| \tilde{u}_L | 541 | 1806 | 1396 | 661 | 1291 |
| \tilde{t}_1 | 390 | 1391 | 1018 | 429 | 846 |
| $\tilde{\chi}_2^0$ | 184 | 756 | 497 | 153 | 328 |
| \tilde{e}_L | 220 | 741 | 818 | 522 | 1039 |
| $\tilde{\tau}_1$ | 99 | 442 | 641 | 440 | 892 |
| $\tilde{\chi}_1^0$ | 98 | 395 | 259 | 81 | 171 |
| $\text{Br}(\tilde{g} \rightarrow \tilde{t}_1 t + \tilde{b}_1 b)$ | 47.0 | 58.4 | 91.1 | 87.8 | 85.9* |
| $\text{Br}(\tilde{q}_R \rightarrow \tilde{\chi}_1^0 q)$ | 98.4 | 99.9 | 99.7 | 8 – 25 | 6 – 21 |
| $\text{Br}(\tilde{q}_R \rightarrow \tilde{g} q)$ | 0 | 0 | 0 | 75 – 92 | 79 – 94 |
| $\text{Br}(\tilde{\chi}_2^0 \rightarrow \tilde{\tau}_{1,2} \tau)$ | 99.6 | 65.5 | 0** | 2.6** | 0** |
| $\text{Br}(\tilde{\chi}_1^\pm \rightarrow \tilde{\tau}_{1,2} \nu, \tilde{\nu} \tau)$ | 98.9 | 81.2 | 0*** | 10.6*** | 0*** |
| $\text{Br}(\tilde{\chi}_2^0 \rightarrow h) \cdot \text{Br}(h \rightarrow b\bar{b})$ | 0 | 8 | 70 | 22.8**** | 68 |

* $\text{Br}(\tilde{g} \rightarrow \tilde{\chi} t(b)t(b))$

** $\text{Br}(\tilde{\chi}_2^0 \rightarrow \tilde{\chi}_1^0 \tau \tau)$

*** $\text{Br}(\tilde{\chi}_1^\pm \rightarrow \tilde{\chi}_1^0 \tau \nu)$

**** $\text{Br}(\tilde{\chi}_2^0 \rightarrow \tilde{\chi}_1^0 b\bar{b})$

5 Generalization for MSSM

The considerations of the previous section can be extended to the case of more the more general MSSM model. One can deduce from Table 1 that if $m_{\tilde{\chi}_2^0, \tilde{\chi}_1^\pm} > m_{\tilde{\tau}_1}$ and $\tan\beta$ is high enough, one can expect an abundant production of taus in the MSSM final states, as in points (130,240) and (400,900) in Table 1. This is illustrated by MSSM points 1 and 2 in Table 3.

Then, if $\tilde{\chi}_2^0 \rightarrow \tilde{\chi}_1^0 h$ decay is kinematically allowed and production of $\tilde{\chi}_2^0$ is significant (both in squark-gluino cascades or just in chargino-neutralino pair production, the latter has important effect if $m_{\tilde{\chi}_2^0, \tilde{\chi}_1^\pm} \ll \min(m_{\tilde{g}}, m_{\tilde{q}})$ and corresponds to the high values of $m_{1/2}$ in mSUGRA), then it results in a noticeable production of b-jets coming from lightest Higgs decay into $b\bar{b}$, see point 3 in Tables 1 – 3, generalizing in MSSM the observations done in [5].

Finally, if $m_{\tilde{q}} > m_{\tilde{g}}$, it enhances mostly the yield of b-quarks, despite the known decrease of $\tilde{\chi}_2^0$ production (with a corresponding decrease of the $h \rightarrow b\bar{b}$ as a source of b-jets) due to the fact that squarks decay through gluino + quarks and the source of $\tilde{\chi}_2^0$ from $\tilde{q} \rightarrow \tilde{\chi}_2^0 q$ is reduced. In this case b-jets are mainly produced in the decays of gluinos, which are, in turn, produced by both left and right squarks. One can compare the points 4 and 5 in Tables 1 – 3.

For the particular choice of MSSM parameters in Table 3, the $\text{Br}(\tilde{g} \rightarrow \tilde{\chi} t(b)t(b))$ in the MSSM case is smaller than that of a similar point of mSUGRA, due to the fact that in mSUGRA \tilde{t}_1 and \tilde{b}_1 are much lighter than all other squarks, whereas in MSSM point 5 only \tilde{b}_1 is a bit lighter (1280 GeV) than other squarks (~ 1300

Table 2: Characteristic features of 5 mSUGRA points. Intermediate $\tan\beta$ case .

| Mass of sparticles (GeV) or Branchings (%) | $(m_0, m_{1/2})$ values for $\tan\beta = 10, \mu > 0, A_0=0$ | | | | |
|--|--|----------------|----------------|----------------|-----------------|
| | 1 (130,240) | 2 (400,900) | 3 (700,600) | 4 (500,200) | 5 (1000,400) |
| \tilde{g} | 604 | 2015 | 1426 | 537 | 1012 |
| \tilde{u}_L | 544 | 1808 | 1393 | 661 | 1291 |
| \tilde{t}_1 | 388 | 1386 | 1016 | 429 | 844 |
| $\tilde{\chi}_2^0$ | 182 | 755 | 498 | 153 | 328 |
| \tilde{e}_L | 220 | 741 | 816 | 522 | 1039 |
| $\tilde{\tau}_1$ | 159 | 522 | 730 | 502 | 1003 |
| $\tilde{\chi}_1^0$ | 97 | 395 | 259 | 80 | 170 |
| $\text{Br}(\tilde{g} \rightarrow \tilde{t}_1 t + \tilde{b}_1 b)$ | 37.0 | 53.5 | 80.0 | 34.0* | 84.0* |
| $\text{Br}(\tilde{q}_R \rightarrow \tilde{\chi}_1^0 q)$ | 98.2 | 99.9 | 99.7 | 8 – 25 | 6 – 20 |
| $\text{Br}(\tilde{q}_R \rightarrow \tilde{g} q)$ | 0 | 0 | 0 | 75 – 92 | 78 – 93 |
| $\text{Br}(\tilde{\chi}_2^0 \rightarrow \tilde{\tau}_{1,2} \tau)$ | 84.8 | 21.0 | 0** | 2.1** | 0** |
| $\text{Br}(\tilde{\chi}_1^\pm \rightarrow \tilde{\tau}_{1,2} \nu, \tilde{\nu} \tau)$ | 68.3 | 32.9 | 0*** | 10.7*** | 0*** |
| $\text{Br}(\tilde{\chi}_2^0 \rightarrow h) \cdot \text{Br}(h \rightarrow b\bar{b})$ | 0 | 26.0 | 74.0 | 18.6**** | 74.0 |

* $\text{Br}(\tilde{g} \rightarrow \tilde{\chi} t(b)t(b))$

** $\text{Br}(\tilde{\chi}_2^0 \rightarrow \tilde{\chi}_1^0 \tau \tau)$

*** $\text{Br}(\tilde{\chi}_1^\pm \rightarrow \tilde{\chi}_1^0 \tau \nu)$

**** $\text{Br}(\tilde{\chi}_2^0 \rightarrow \tilde{\chi}_1^0 b\bar{b})$

GeV), but $\tilde{b}_2, \tilde{t}_{1,2}$ are heavier (1320, 1307 and 1309 GeV respectively). But if in MSSM the third generation squarks are, as in mSUGRA, significantly lighter than first two generation squarks, it immediately results in the increase of $\text{Br}(\tilde{g} \rightarrow \tilde{\chi} t(b)t(b))$ up to values of 80-90 %, as in mSUGRA. In the MSSM domain explored so far, masses of charginos and neutralinos are obtained still assuming universal gaugino mass at the GUT scale. The common slepton masses are taken fairly arbitrary in such a way that $m_{\tilde{\chi}_1^0} < m_{\tilde{\tau}_1} < m_{\tilde{\chi}_2^0}$.

6 Results and conclusions

Our findings are summarized in Figs.8 – 10 where we plot the probabilities to find at least 1, 3 or 5 b-jets *per event* respectively (with $E_T^b > 50$ GeV in $|\eta^b| < 2.4$) over mSUGRA parameter space for various sets of $\tan\beta$, $\text{sign}(\mu)$. Even the probabilities for 3 b-jets *per event* within CMS acceptance (and with $E_T^b > 50$ GeV !) are significant for all $\tan\beta$ over most of parameter space, from a few % to ~ 40 %, the region $m_0 > m_{1/2}$ being the richest one. One can see that the effect of b Yukawa couplings increase with $\tan\beta$ is visible only in Fig.10, i.e. asking at least 5 b-jets per event. We would like to emphasize that the exceptionally large probability per event to find a b-jet in a SUSY event is not limited to large $m_0, m_{1/2}$ (i.e. large \tilde{g}, \tilde{q} values), but *is valid throughout the whole plane, i.e. even for \tilde{g}, \tilde{q} masses ~ 500 GeV, just above the Tevatron reach*, as illustrated by columns 1 and 4 in Tables 1,2.

The same probability distributions for at least 1, 2 and 3 taus *per event* are shown in Figs.11 – 13 respectively (again for $E_T^\tau > 50$ GeV in $|\eta^\tau| < 2.4$). Here one can see a much more pronounced difference

Table 3: Characteristic features of 5 MSSM points.

| Mass of sparticles (GeV) or Branchings (%) | $\tan\beta = 35, \mu = 500 \text{ GeV}, m_A = 1000 \text{ GeV}, A_t=A_b=A_\tau=0$ | | | | |
|--|---|------|------|----------|---------|
| | 1 | 2 | 3 | 4 | 5 |
| \tilde{g} | 600 | 2000 | 1400 | 500 | 1000 |
| \tilde{q} | 500 | 1800 | 1300 | 650 | 1300 |
| $\tilde{\chi}_2^0$ | 177 | 485 | 407 | 135 | 279 |
| \tilde{e}_L | 200 | 400 | 700 | 650 | 1300 |
| $\tilde{\tau}_1$ | 107 | 362 | 679 | 628 | 1288 |
| $\tilde{\chi}_1^0$ | 91 | 319 | 218 | 69 | 145 |
| $\text{Br}(\tilde{g} \rightarrow \tilde{t}_1 t + \tilde{b}_1 b)$ | 23.3 | 31.8 | 21.6 | 17.8* | 36.5* |
| $\text{Br}(\tilde{q}_R \rightarrow \tilde{\chi}_1^0 q)$ | 99.9 | 96.8 | 98.7 | 5 – 17 | 5 – 18 |
| $\text{Br}(\tilde{q}_R \rightarrow \tilde{g} q)$ | 0 | 0 | 0 | 83 – 95 | 81 – 94 |
| $\text{Br}(\tilde{\chi}_2^0 \rightarrow \tilde{\tau}_{1,2} \tau)$ | 100.0 | 40.5 | 0** | 1.8** | 0** |
| $\text{Br}(\tilde{\chi}_1^\pm \rightarrow \tilde{\tau}_{1,2} \nu, \tilde{\nu} \tau)$ | 99.8 | 45.3 | 0*** | 10.0*** | 0*** |
| $\text{Br}(\tilde{\chi}_2^0 \rightarrow h) \cdot \text{Br}(h \rightarrow b\bar{b})$ | 0 | 26.1 | 72.0 | 21.8**** | 65.9 |

* $\text{Br}(\tilde{g} \rightarrow \tilde{\chi} t(b)t(b))$

** $\text{Br}(\tilde{\chi}_2^0 \rightarrow \tilde{\chi}_1^0 \tau \tau)$

*** $\text{Br}(\tilde{\chi}_1^\pm \rightarrow \tilde{\chi}_1^0 \tau \nu)$

**** $\text{Br}(\tilde{\chi}_2^0 \rightarrow \tilde{\chi}_1^0 b\bar{b})$

between various values of $\tan\beta$ already with at least one tau in the final state (Fig.11). The clearly visible ridge on the $m_0, m_{1/2}$ plane corresponds to the mSUGRA domains of parameter space where $\tilde{\chi}_2^0$ and $\tilde{\chi}_1^\pm$ decay into sleptons. The ridge becomes more and more pronounced as $\tan\beta$ increases thanks to increasing τ Yukawa couplings and decreasing τ mass relative to \tilde{e} and $\tilde{\mu}$. One can also notice a significant (15 – 20 %) level of tau production throughout the $m_0, m_{1/2}$ plane, mainly from W and b-jets.

It is also clear from the comparison of Figs.8 – 10 with Figs.11 – 13 that the domains of parameter space where taus and b-jets are produced abundantly are complementary, but together cover most of parameter space ! It will thus be of utmost importance to have a high performance microvertex device to disentangle the complicated final states (Figs.4 – 7) through b and τ tagging, and the more so the higher is $\tan\beta$; whether $\tan\beta$ is large can be detected already in early LHC running through the modifications of the expected shape of opposite sign dilepton mass spectra discussed in ref [11] and due precisely to the increased τ production. In general, the importance of the b-tagging capability of CMS increases with the SUSY mass scale whatever $\tan\beta$ due to complexification of the final states with increasing masses, but it is already of crucial importance in the mass range just beyond the Tevatron II reach, $m_{\tilde{g}}, m_{\tilde{q}} \gtrsim 400 \text{ GeV}$, i.e. $m_0 \gtrsim 200 \text{ GeV}$, $m_{1/2} \gtrsim 400 \text{ GeV}$ in this model (Tables 1 – 3 and Figs.8 – 10).

The main conclusions of our study are the following.

It has been known quantitatively for a long time that b-tagging will be important for SUSY studies. Our investigations further strengthen this feeling. Within the mSUGRA model we find surprisingly high probabilities per event, in the few tens of %, to find hard b-jets within CMS acceptance, even for multiple-b final states, the effect increasing moderately with $\tan\beta$. What is more spectacular and not so well known and appreciated, is the rapid increase of τ -probability and multi- τ probability per event with increasing $\tan\beta$. Furthermore, there is an almost complete complementarity in parameter space coverage by those two

experimental signatures. This implies that a high performance microvertex detector will be essential for SUSY event analysis, especially if $\tan\beta \geq 10$, and the more so more massive are the squarks and gluinos. Every effort should thus be made to have a third pixel layer in the CMS tracker to have redundancy and a safety margin to ensure in the impact parameter measurements. At least provisions must be made in the inner tracker mechanical design and beam pipe design that this third layer can be inserted if SUSY shows up at the LHC *rendes-vous*. Also every effort should be made to keep the innermost pixel layer at 4 cm radius even in high luminosity conditions, where probably frequent replacements will be needed, as it improves significantly the b-tagging performance of CMS as investigations in ref. [6, 12] have shown. It is also only with high luminosity that the highest masses are attainable, and it is for these masses that the decays are most complicated and b-tagging most useful.

An objection can be raised to these conclusions, namely that they are based on a very specific SUSY scenario - mSUGRA. However, these conclusions will be generally true in whatever SUSY model as long as \tilde{t}_1 or \tilde{b}_1 are substantially lighter than the remaining squarks, and the $\tilde{\tau}$ is lighter than $\tilde{\chi}_2^0$ and/or $\tilde{\chi}_1^\pm$ and $\tilde{\tau}_1$ is not significantly heavier than other sleptons, as was discussed in section 5. Some preliminary results in the more general MSSM context have already been shown, and those investigations are being actively pursued at present.

References

- [1] H. Baer, C.-H. Chen, F. Paige and X. Tata, Phys.Rev. **D52** (1995) 2746; Phys.Rev. **D53** (1996) 6241; CMS collaboration (S.Abdullin *et al.*), CMS NOTE 1998/006, hep-ph/9806366; S. Abdullin and F. Charles, Nucl.Phys. **B547** (1999) 60.
- [2] H. Baer, C.-H. Chen, F. Paige and X. Tata, Phys.Rev. **D50** (1994) 4508 ; I. Iachvili and A.Kharchilava, Nucl.Phys. **B526** (1998) 153; D. Denegri, W. Majerotto and L. Rurua, Phys.Rev. **D58** (1998) 095010.
- [3] H.Baer *et al.*, Phys.Rev. **D58** (1998) 075008.
- [4] CMS collaboration, *Technical Proposal*, CERN/LHCC 94-38.
- [5] S. Abdullin and D. Denegri, CMS NOTE 1997/070; V. Drollinger, presentations at CMS physics meetings 1998-99.
- [6] CMS Tracker TDR : The Tracker Project, CERN/LHCC 98-6, CMS TDR-5, April 1998.
- [7] R. Kinnunen, A. Nikitenko, CMS NOTE 1997/002.
- [8] H. Baer *et al.*, Phys.Rev. **D51** (1995) 1046.
- [9] H. Baer and M.Brhlík, Phys.Rev. **D57** (1998) 567.
- [10] F. Paige and S. Protopopescu, in *Supercollider Physics*, p. 41, ed. D. Soper (World Scientific, 1986); H. Baer, F. Paige, S. Protopopescu and X. Tata, in *Proceedings of the Workshop on Physics at Current Accelerators and Supercolliders*, ed. J. Hewett, A. White and D. Zeppenfeld (Argonne National Laboratory, 1993).
- [11] D. Denegri, W. Majerotto and L. Rurua, CMS NOTE 1998/085, hep-ph/9901231, accepted for publication in Phys.Rev. **D** .
- [12] A. Caner, S. Banerjee, A. Khanov and N. Stepanov, CMS tracker optimisation studies, CMS working group meetings 1998-99; A. Caner, S. Banerjee, A. Khanov and N. Stepanov, "Track and vertex Finding Performance with CMS Inner Tracker", presented at the 7th Int. Workshop on vertex Detectors, Santorini, Greece, Sept. 98; accepted for publication by NIM A.

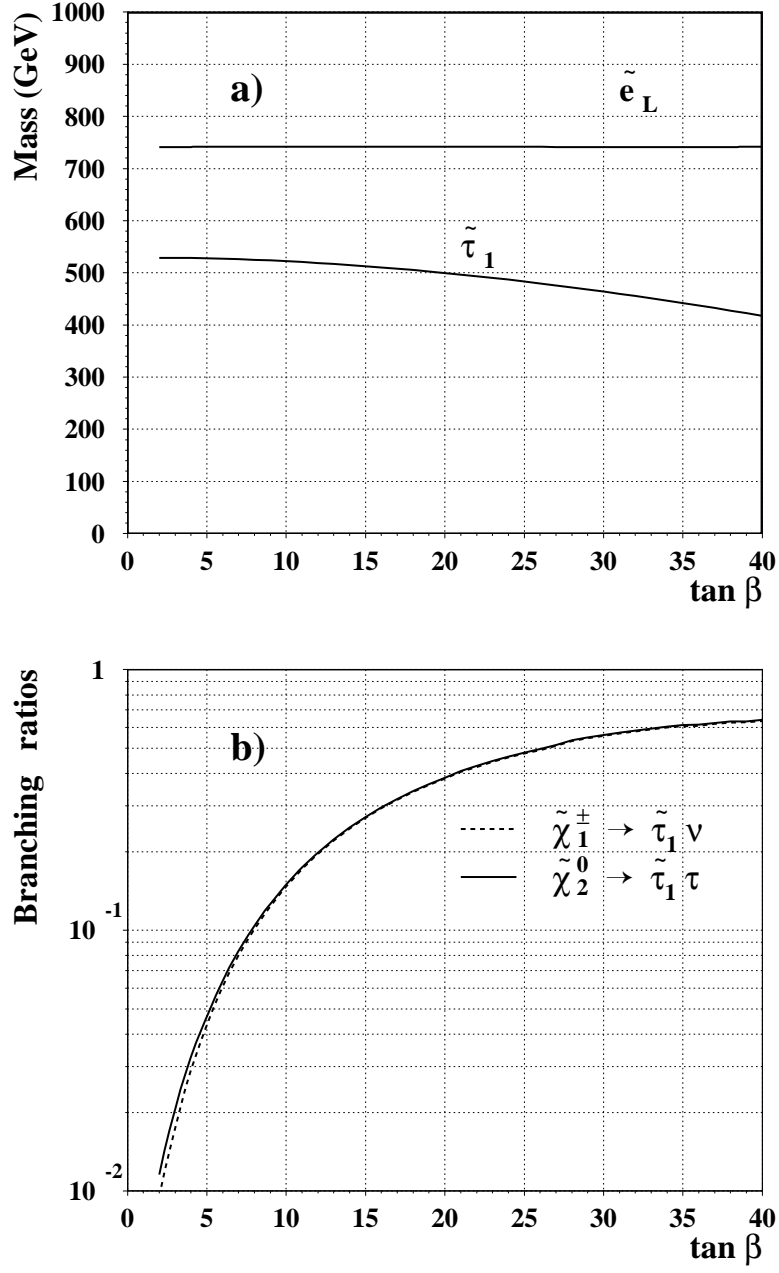
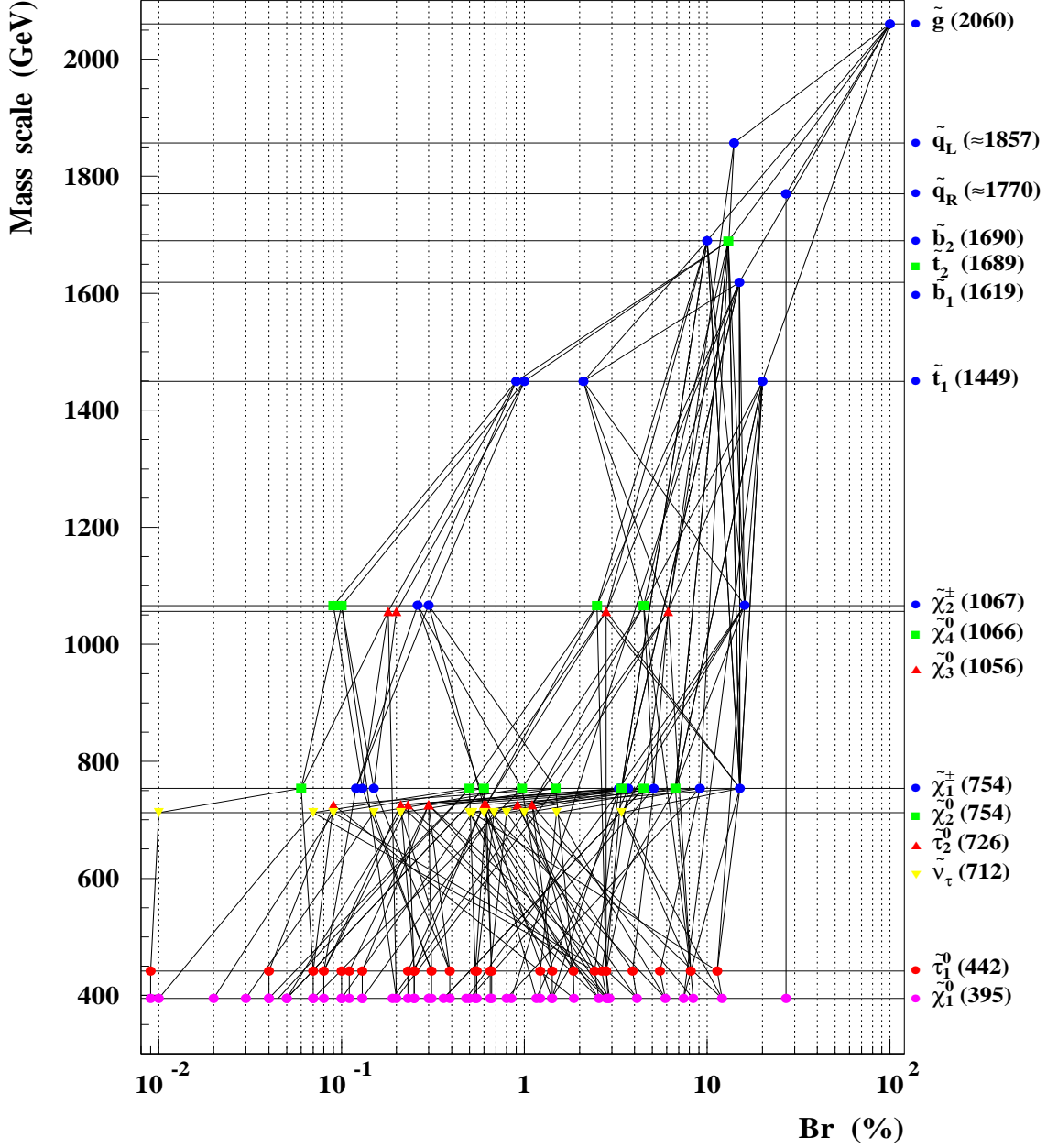


Figure 3: a) Masses of left selectron (\tilde{e}_L) and lightest stau ($\tilde{\tau}_1$) vs $\tan \beta$, b) branching ratios of lightest chargino ($\tilde{\chi}_1^\pm$, dashed line) and next-to-lightest neutralino ($\tilde{\chi}_2^0$, solid line) into final states with lightest stau as a function of $\tan \beta$ for $m_0=400$ GeV, $m_{1/2}=900$ GeV, $A_0=0$ and $\mu > 0$.



| | | | |
|------------------------------------|----------|-----------------------------------|---------|
| $\tilde{\chi}_1^0$ qq | (27.0 %) | $\tilde{\chi}_1^0$ $\tau\nu WWbb$ | (4.1 %) |
| $\tilde{\chi}_1^0$ $\tau\nu Wbb$ | (12.1 %) | $\tilde{\chi}_1^0$ $\tau\tau bb$ | (2.9 %) |
| $\tilde{\chi}_1^0$ $\tau\tau WWbb$ | (8.4 %) | $\tilde{\chi}_1^0$ $\tau\tau qq$ | (2.9 %) |
| $\tilde{\chi}_1^0$ $WWbb$ | (7.4 %) | $\tilde{\chi}_1^0$ $\tau\nu ZWbb$ | (2.8 %) |
| $\tilde{\chi}_1^0$ $\tau\nu qq$ | (5.9 %) | $\tilde{\chi}_1^0$ $\tau\nu hWbb$ | (2.6 %) |

Figure 4: Typical decay modes for massive (2060 GeV) gluino for **high $\tan\beta = 35$** ($m_0 = 400$ GeV, $m_{1/2} = 900$ GeV, $A_0 = 0$ and $\mu > 0$). The ten largest individual decay modes are specified. Note multiplicity of b and τ final states.

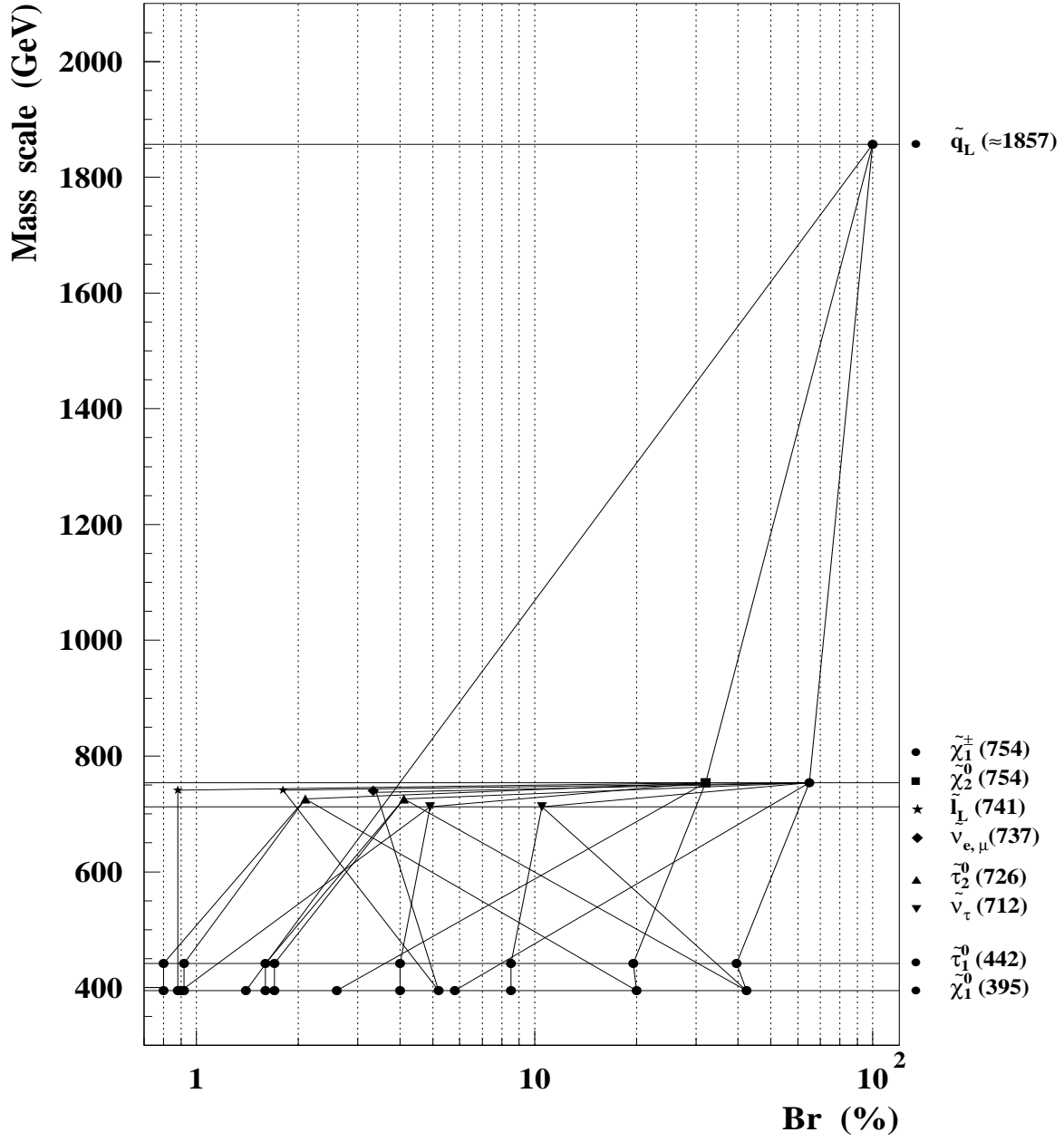
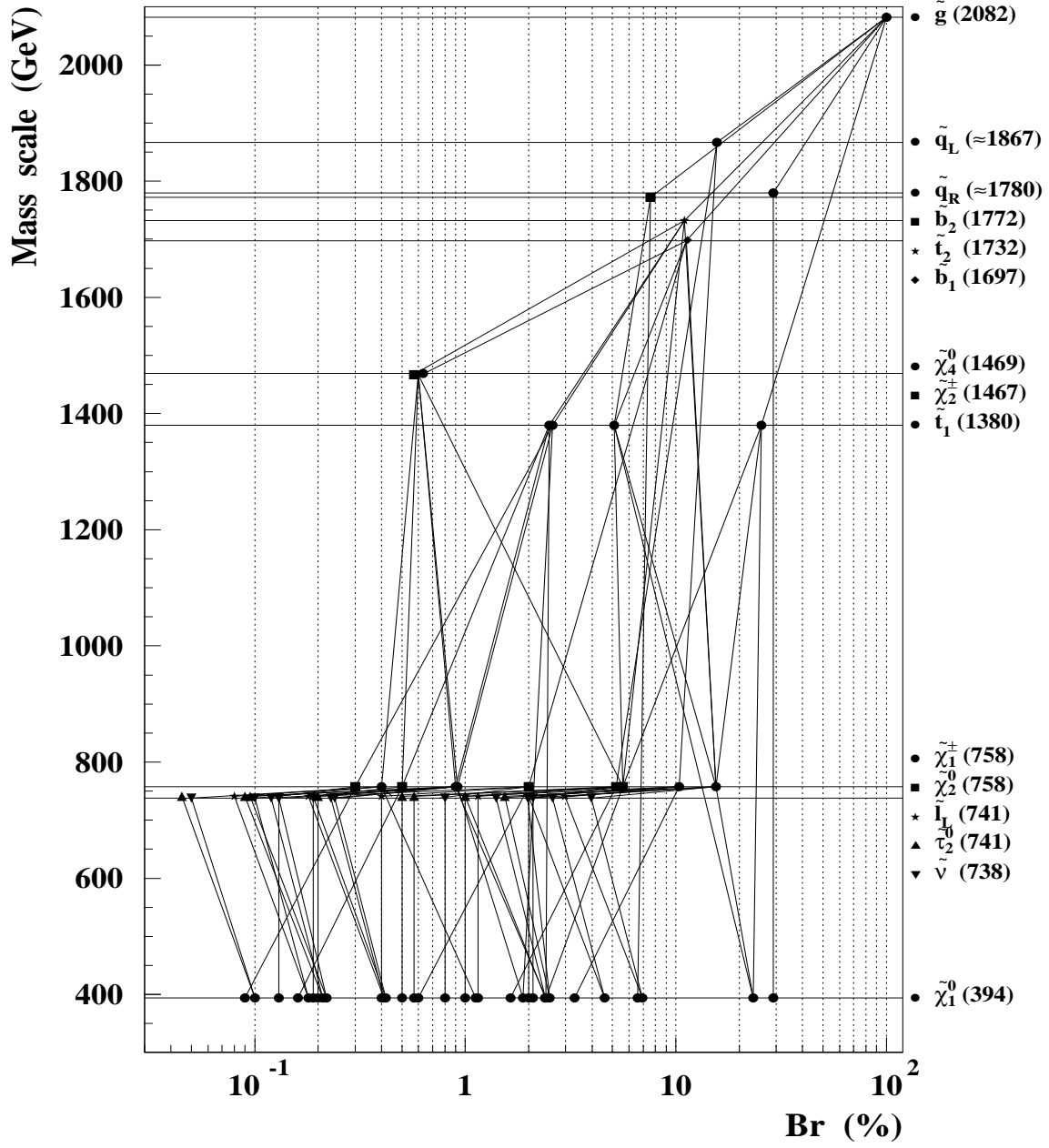


Figure 5: Typical decay modes for massive (1857 GeV) left squark for high $\tan\beta = 35$ ($m_0 = 400$ GeV, $m_{1/2} = 900$ GeV, $A_0 = 0$ and $\mu > 0$).



| | | | |
|--------------------------|----------|----------------------------------|---------|
| $\tilde{\chi}_1^0$ qq | (29.0 %) | $\tilde{\chi}_1^0$ Wqq | (3.3 %) |
| $\tilde{\chi}_1^0$ WWbb | (23.3 %) | $\tilde{\chi}_1^0$ τ vWbb | (2.5 %) |
| $\tilde{\chi}_1^0$ lvWbb | (6.9 %) | $\tilde{\chi}_1^0$ h WWbb | (2.4 %) |
| $\tilde{\chi}_1^0$ bb | (6.6 %) | $\tilde{\chi}_1^0$ τ vqq | (2.4 %) |
| $\tilde{\chi}_1^0$ lvqq | (4.6 %) | $\tilde{\chi}_1^0$ $\nu\nu$ WWbb | (2.2 %) |

Figure 6: Typical decay modes for massive (2082 GeV) gluino for low $\tan\beta = 2$ ($m_0 = 400$ GeV, $m_{1/2} = 900$ GeV, $A_0 = 0$ and $\mu > 0$). Note again large number of final states with b's.

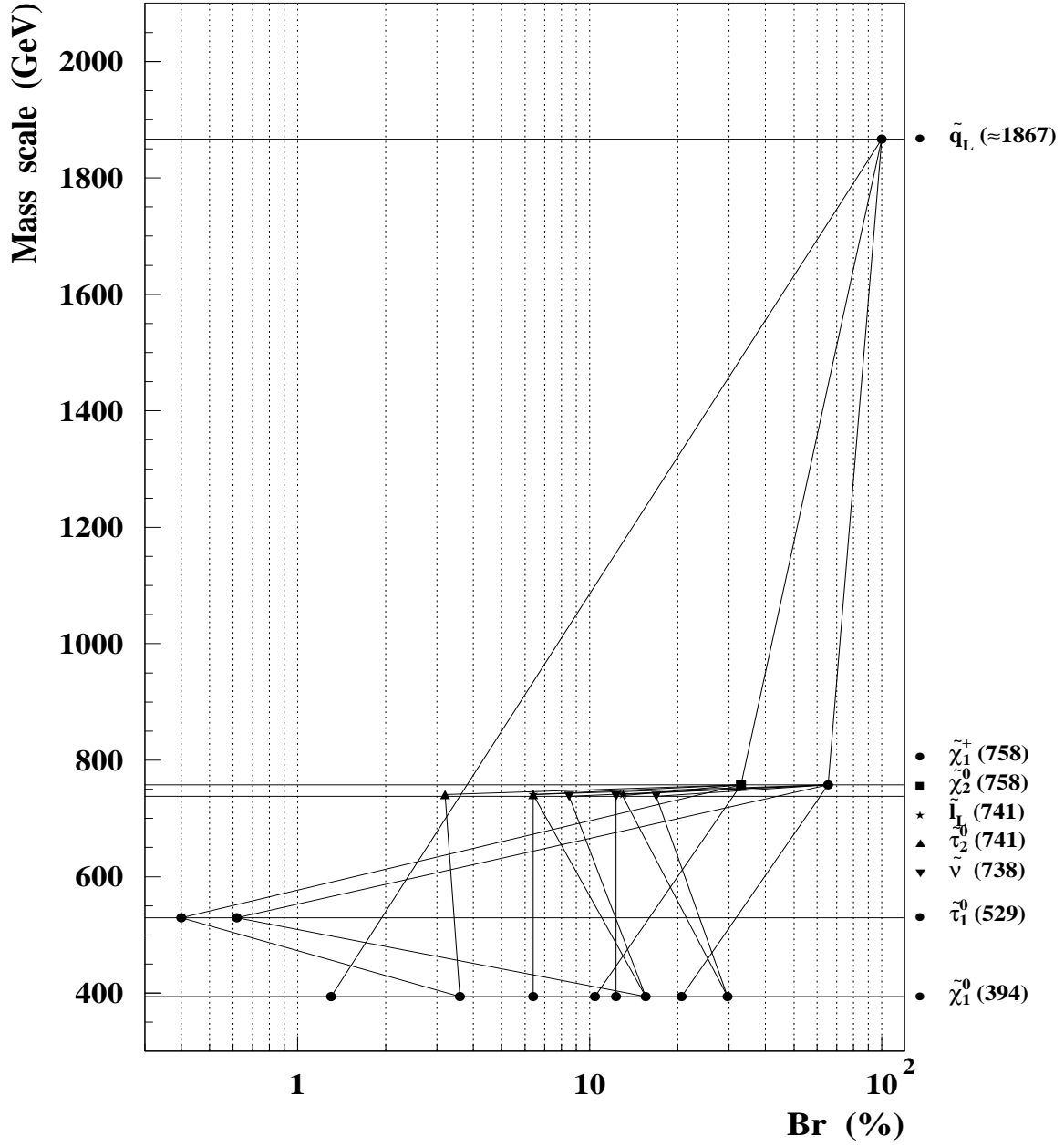


Figure 7: Typical decay modes for massive (1867 GeV) left squark for low $\tan\beta = 2$ ($m_0 = 400$ GeV, $m_{1/2} = 900$ GeV, $A_0 = 0$ and $\mu > 0$).

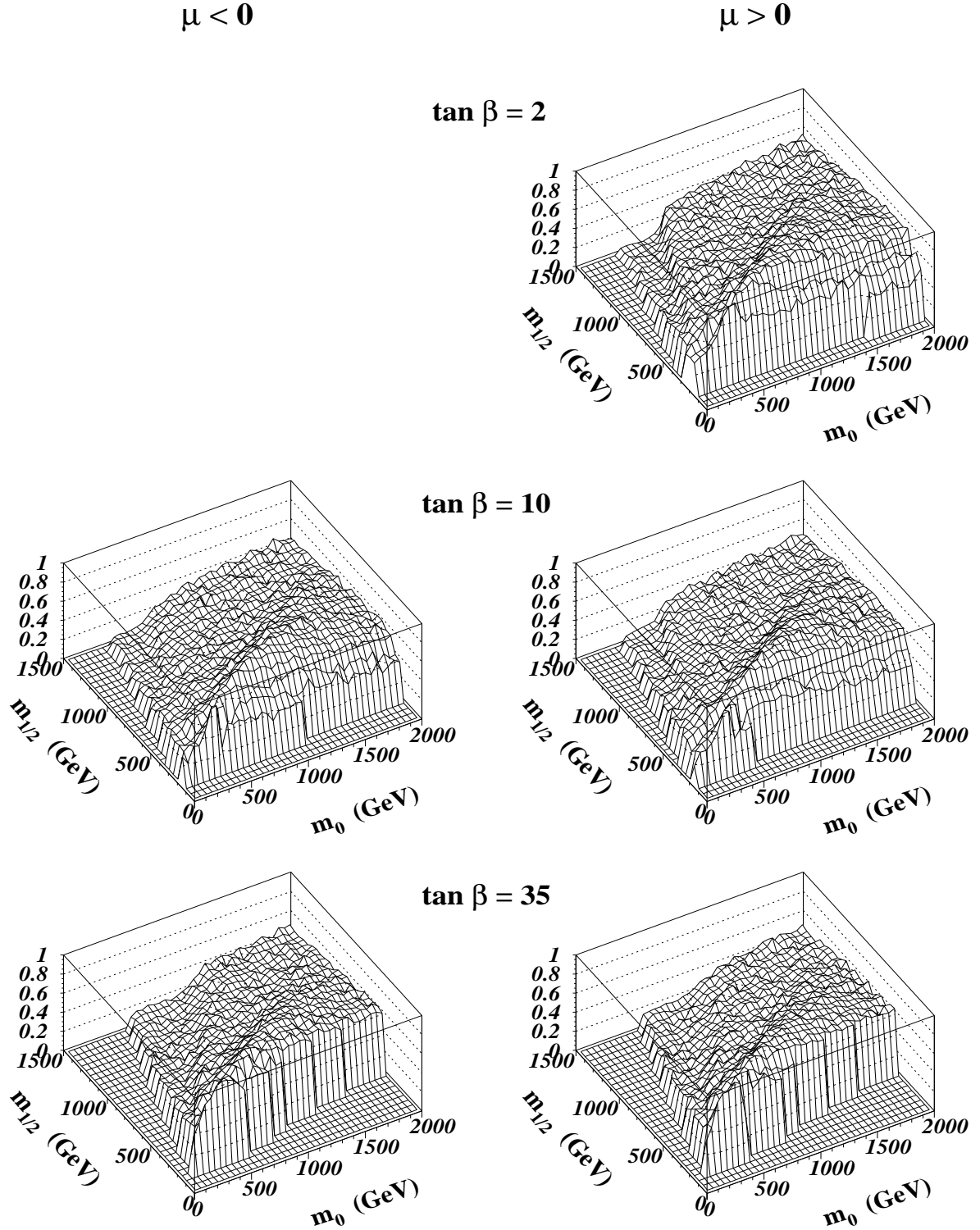


Figure 8: Probability to find at least one b-jet per event with $E_T^b > 50$ GeV in CMS acceptance $|\eta^b| < 2.4$ for various mSUGRA parameter domains. Notice large probability for all $\tan\beta$ and μ and over all explorable $m_0, m_{1/2}$ domain.

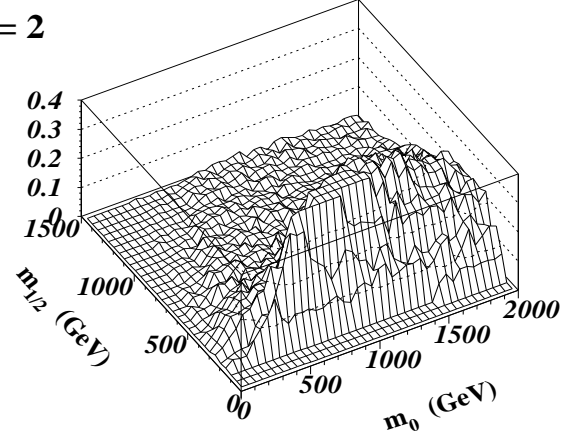
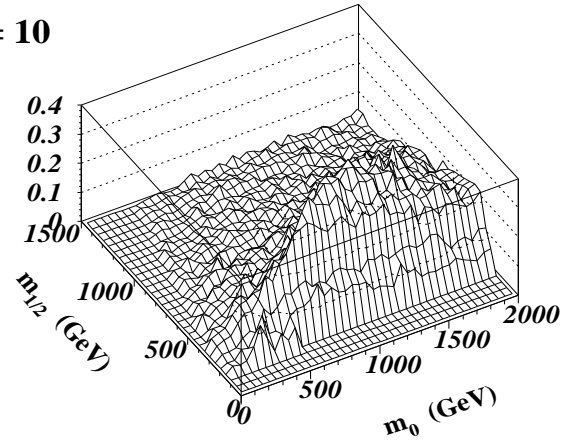
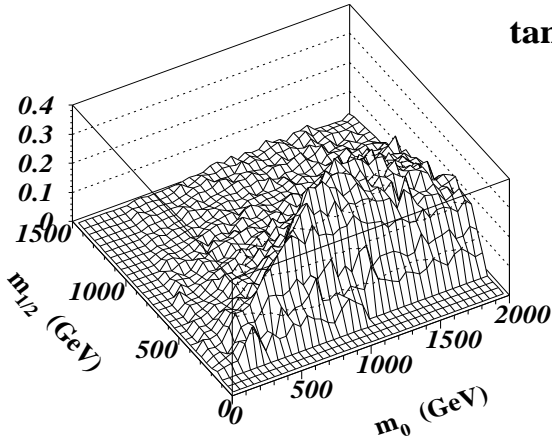
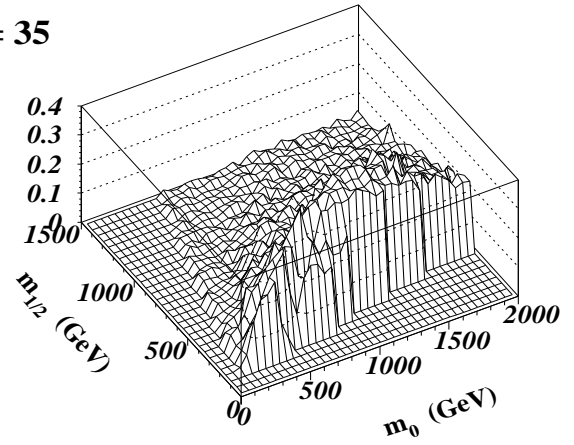
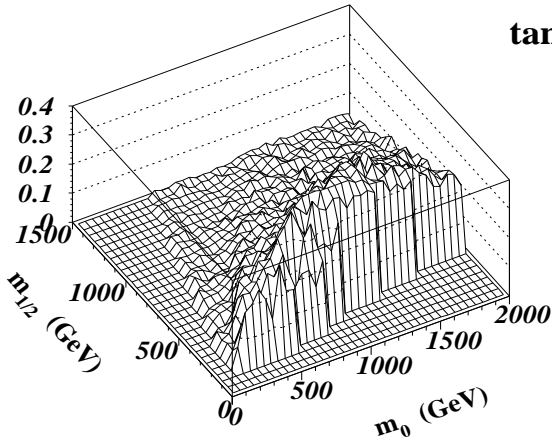
$\mu < 0$ $\mu > 0$ $\tan \beta = 2$  $\tan \beta = 10$  $\tan \beta = 35$ 

Figure 9: Same as in Fig.8, but for at least 3 b-jets.

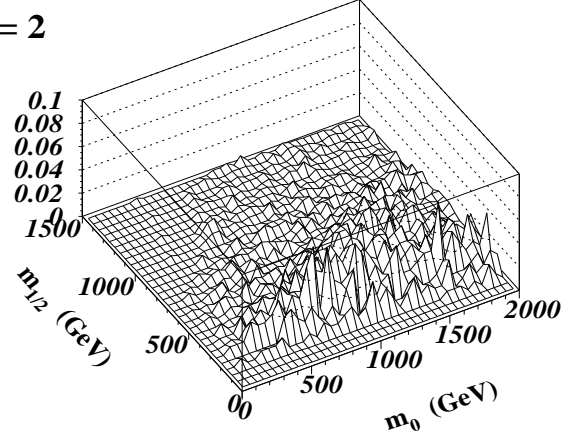
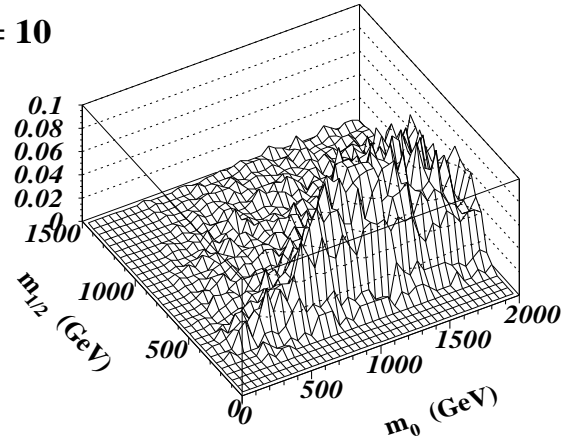
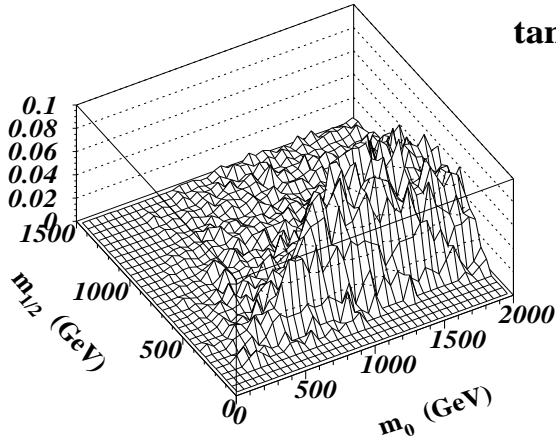
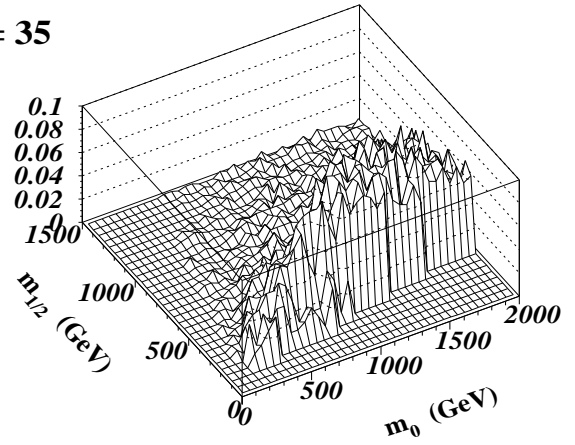
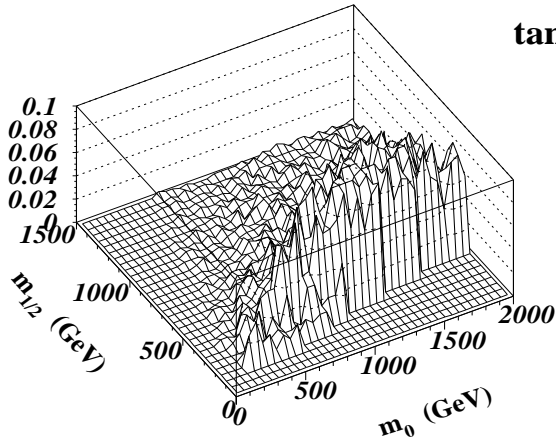
$\mu < 0$ $\mu > 0$ $\tan \beta = 2$  $\tan \beta = 10$  $\tan \beta = 35$ 

Figure 10: Same as in Fig.8, but for at least 5 b-jets.

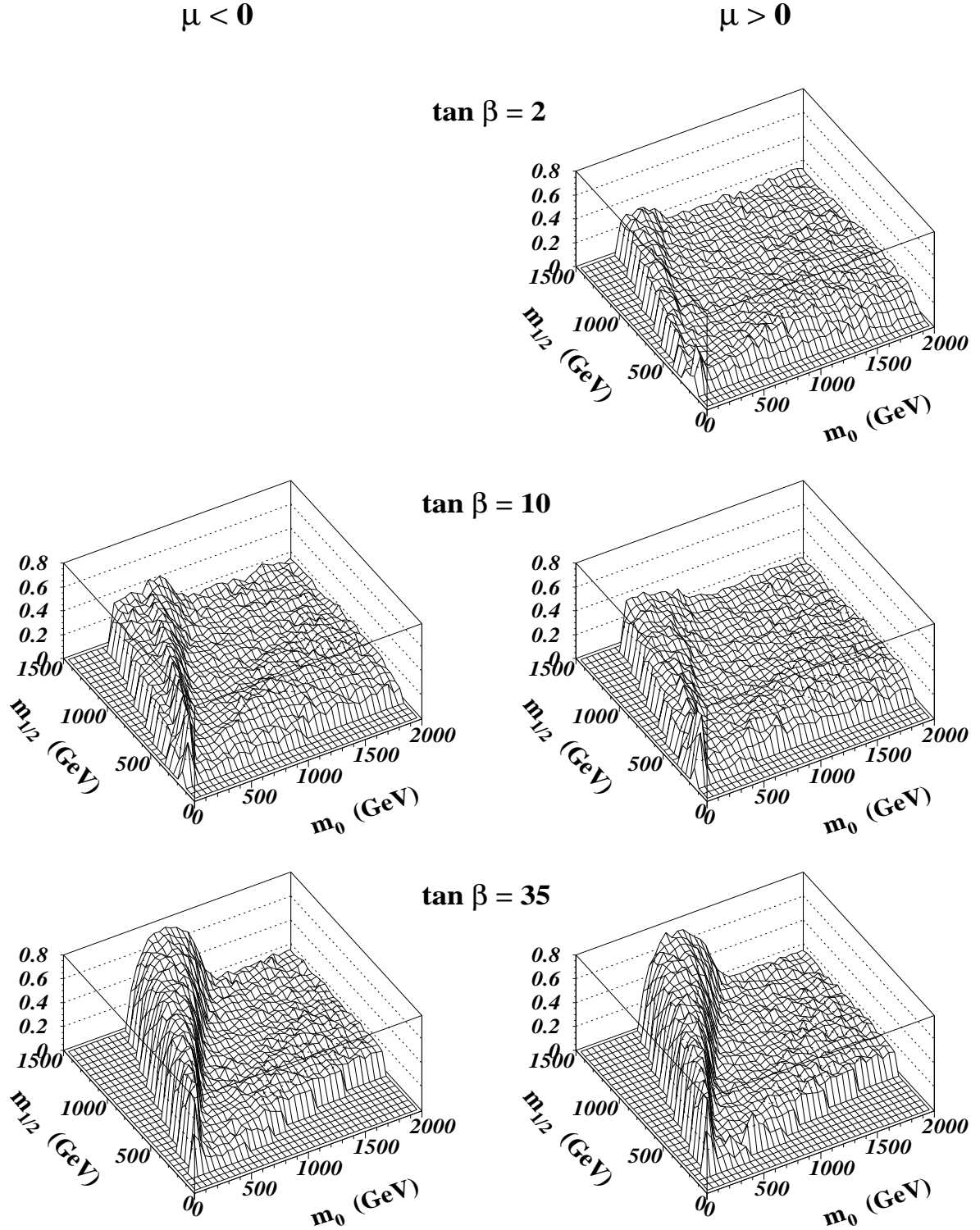


Figure 11: Probability to find at least one tau per event with $E_T^\tau > 50$ GeV in CMS acceptance $|\eta^\tau| < 2.4$ for various mSUGRA parameter domains. Note large increase with increasing $\tan \beta$, but significant probability nonetheless throughout parameter space.

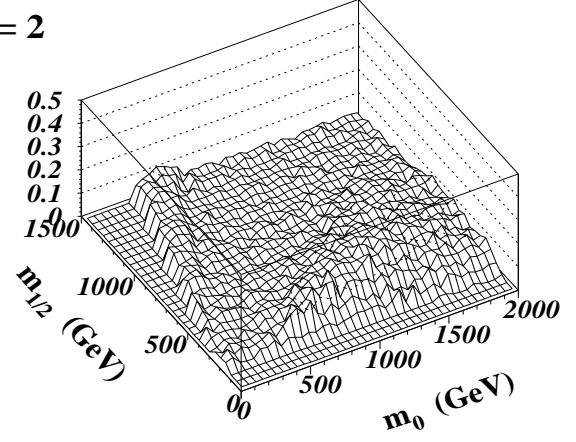
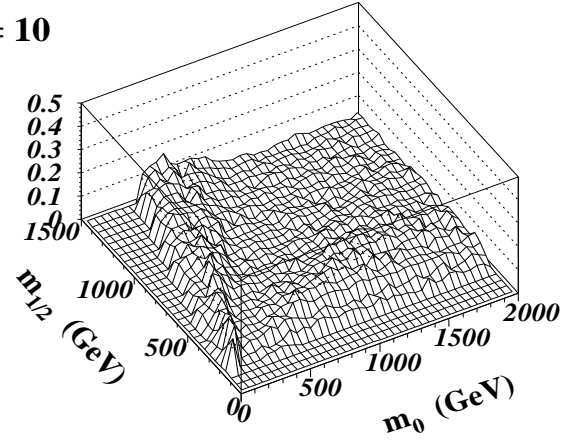
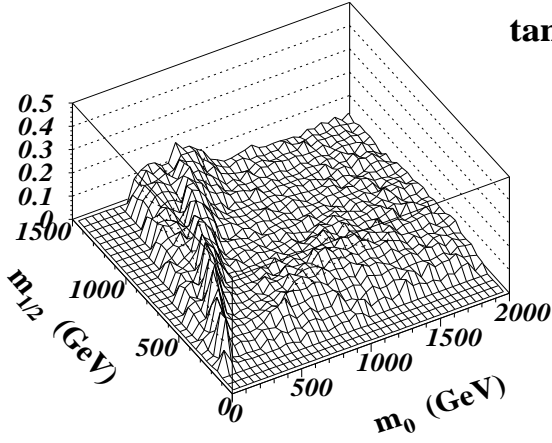
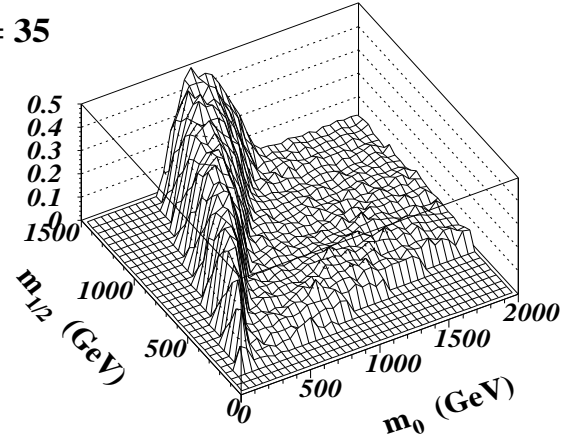
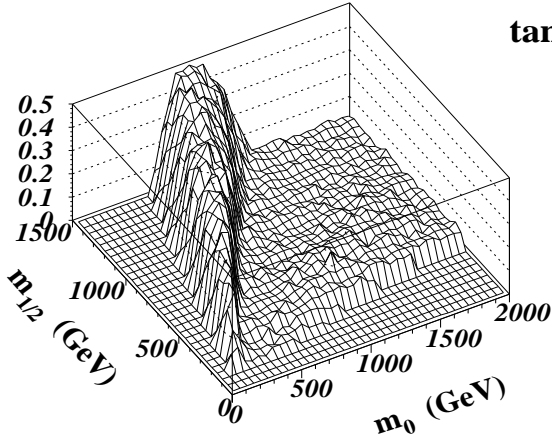
$\mu < 0$ $\mu > 0$ $\tan \beta = 2$  $\tan \beta = 10$  $\tan \beta = 35$ 

Figure 12: Same as in Fig.11, but for at least 2 taus.

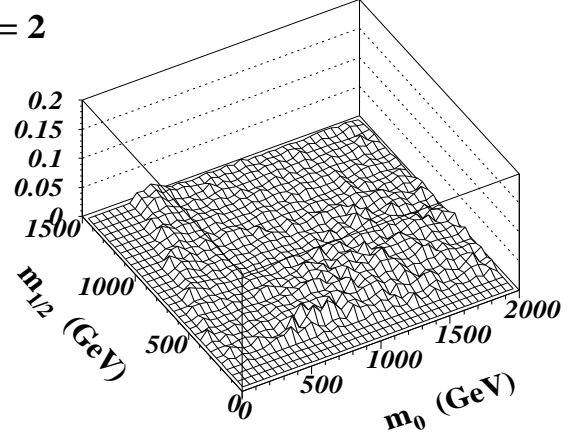
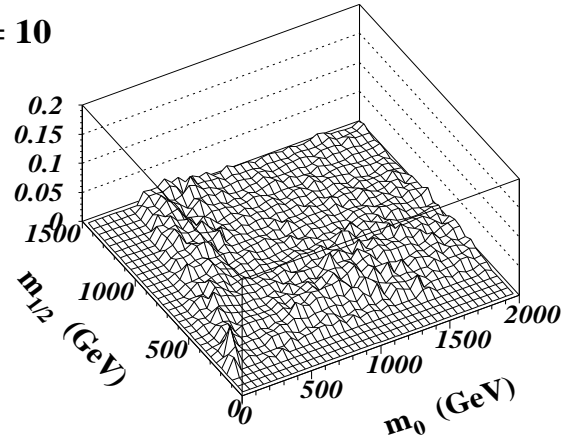
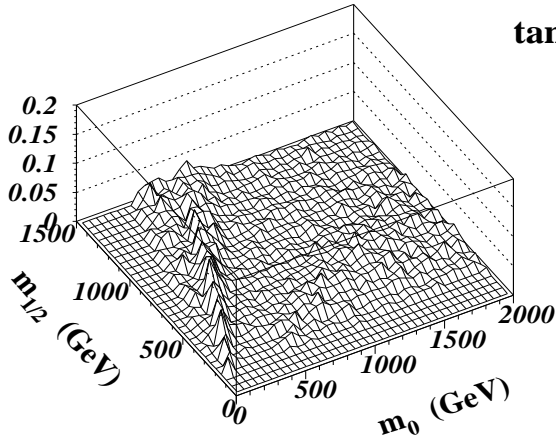
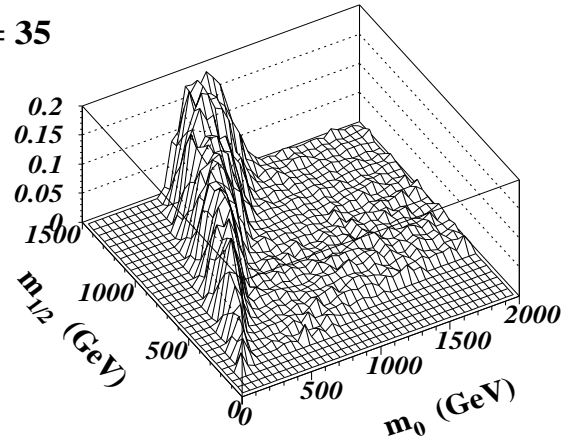
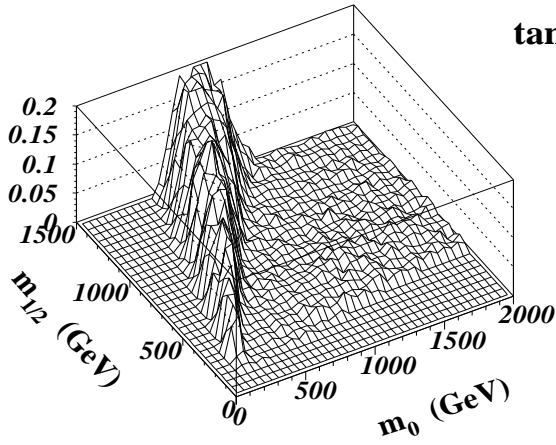
$\mu < 0$ $\mu > 0$ $\tan \beta = 2$  $\tan \beta = 10$  $\tan \beta = 35$ 

Figure 13: Same as in Fig.11, but for at least 3 taus.